Evidence for Line Nodes in the Superconducting Gap of $K_{1-x}Na_xFe_2As_2$ ($x = 0, 0.1$) Single Crystals from Low-Temperature Specific-Heat Measurements

M. Abdel-Hafiez*,[1] V. Grinenko*,[1] S. Aswartham,[1] I. Morozov†,[1] M. Roslova†,[1] O. Vakaliuk,[1] S.-L. Drechsler,[1,‡] S. Johnston §,[1] D.V. Efremov,[1] J. van den Brink,[1,2] H. Rosner,[3] M. Kumar,[1] C. Hess,[1] S. Wurmehl,[1] A.U.B. Wolter,[1] B. Büchner,[1,4] E.L. Green,[5] J. Wosnitza,[5,2] P. Vogt,[6] A. Reifenberger,[6] C. Enss,[6] and R. Klingeler[6]

[1] *Leibniz-Institute for Solid State and Materials Research, IFW-Dresden, D-01171 Dresden, Germany*
[2] *Institut für Festkörperphysik, TU Dresden, D-01062 Dresden, Germany*
[3] *Max-Planck Institute for Chemical Physics of Solids, D-01187 Dresden, Germany*
[4] *Department of Physics, University of Technology (TU Dresden), D-01062 Dresden, Germany*
[5] *Dresden High Magnetic Field Laboratory, Helmholtz-Zentrum Dresden-Rossendorf, 01314 Dresden, Germany*
[6] *Kirchhoff-Institute for Physics, University of Heidelberg, D-69120 Heidelberg, Germany*

(Dated: January 24, 2013)

From the measurement and analysis of the specific heat of high-quality $K_{1-x}Na_xFe_2As_2$ single crystals we establish the presence of large T^2 contributions with coefficients $\alpha_{sc} \approx 30$ mJ/mol K^3 at low-T for both $x = 0$ and 0.1. This evidences line-nodes in the superconducting gap and suggests d-wave superconductivity on all Fermi-surface sheets with an average gap amplitude of Δ_0 in the range of 0.5 - 0.8 meV. The derived Δ_0 and observed T_c agree well with the values calculated within the Eliashberg-theory, adopting a spin-fluctuation mediated pairing in the intermediate coupling regime.

PACS numbers: 74.25.Bt, 74.25.Dw, 74.25.Jb, 65.40.Ba

In spite of the substantial experimental and theoretical research efforts to elucidate the symmetry and magnitude of the superconducting order parameter for the Fe pnictides [1, 2], important questions concerning the doping evolution of the superconducting gap remain unsolved [3, 4]. In the stoichiometric parent compounds nesting usually occurs between electron (el) and hole (h) Fermi-surface sheets (FSS) which is responsible for the presence of long-range spin density wave (SDW) order. Superconductivity (SC) emerges when the SDW order is suppressed by doping or external pressure [2]. An $s_\pm$ gap symmetry (nodeless gap function with opposite signs of the order parameters for el and h pockets) is believed to be realized in under- and optimally doped compounds, since the antiferromagnetic spin fluctuations (SF) on the vector $Q = (\pi, \pi)$ connecting the el and h pockets remain strong in the vicinity of the SDW phase. The situation in the overdoped regime is not so clear. With further doping, el (h) bands disappear. Therefore, the paradigm of the *SF glue* at the vector $Q = (\pi, \pi)$ does not work. However, SF have been found at some incommensurate propagation vectors [5]. This has led to several proposals for the order parameters in heavily doped compounds: extended s, d, $s + id$ wave [3, 6–8]. Thus, even from theoretical perspective the situation is still controversial.

One of the most interesting families from this point of view is $Ba_{1-x}K_xFe_2As_2$. Superconductivity in this compound occurs at $x \approx 0.15$ [9]. T_c increases with K doping up to $T_c \approx 38$ K for x=0.4 (optimally doped regime). In this region experiments such as angle-resolved photoemission spectroscopy (ARPES) [10] and thermal conductivity [11] show the absence of nodes in the gap, confirming an s-wave character of the order parameter. The overdoped regime is not well studied, so far. The measurements on polycrystalline samples show that T_c monotonically decreases with doping, reaching T_c= 3.5 K for KFe_2As_2 (K122) [9]. Whereas the el pockets are completely gone in K122, it was theoretically proposed that a change of the order-parameter symmetry to d, $s_\pm$ wave with accidental nodes, or $s + id$ should occur [3, 6–8].

Until now, there is no consensus in the interpretation of available experimental data in favor of one of the proposed order parameters. Indeed, measurements of thermal conductivity [12, 13] and of the London penetration depth [14] have been interpreted in terms of d-wave SC with line nodes on each FSS. In contrast, recent ultrahigh-resolution laser ARPES data for K122 have been interpreted in terms of a rather specific *partial* nodal s-wave SC having an unusual gap with "octet line nodes" on the middle FSS, an almost-zero gap on the outer FSS, and a nodeless gap on the inner FSS [15]. The specific-heat (SH) data for K122 above 0.4 K, only, were interpreted within a weak-coupling BCS-like multiple SC gap scenario with line nodes [16, 17], adopting multiband- d- or s- wave nodal SC. But at the same time an extremely strong coupling and/or correlated regimes with heavy quasiparticles were suggested for the normal state. Moreover, the authors of a subsequent SH study in magnetic fields [18] doubted such an interpretation and

*M.A. and V.G. have equally contributed to the present paper.
†Present address: Lomonosov Moscow State University, GSP-1, Leninskie Gory, Moscow, 119991, Russian Federation
§Present address: Dept. of Physics and Astronomy, University of Brit. Columbia, Vancouver, British Columbia, Canada V6T 1Z1

denied the presence of a smaller second gap based on the observation of a non-intrinsic magnetic transition at low-T, probably due to unknown magnetic impurities. Naturally, under such circumstances a T^2 behavior, generic for line nodes in the SC gap [19–21], could not be observed. Hence, further studies using cleaner samples are necessary to clarify the symmetry of the SC order parameter and the magnitude of the coupling strength. These two issues are the main points of the present letter.

$K_{1-x}Na_xFe_2As_2$ single crystals with x=0 (K122) and x=0.1 (K(Na)122) were grown using KAs as a flux. SH data in various fields were obtained by a relaxation technique in a Physical Properties Measurement System (PPMS, Quantum Design). The magnetic ac susceptibility as a function of temperature was also measured by use of the PPMS. The T-dependence of the electrical resistivity was measured using a standard 4-probe DC technique. Two single crystals, K122 and K(Na)122, were selected for SH measurements below 0.4 K using the heat-pulse technique within a dilution refrigerator.

The T-dependence of the volume ac susceptibilities (χ' and χ'') of K122 and K(Na)122 are shown in Fig. 1. The sharp transition with $\sim$ 100 % SC volume fraction confirms the bulk nature of superconductivity and the high quality of our crystals. The T-dependence of the in-plane electrical resistivity evidences a drop to zero at 3.6 K for K122 and at 2.9 K for K(Na)122 in agreement with the diamagnetic onset seen in the χ_{AC} data.

Zero-field specific-heat, C, of K122 and K(Na)122 between 0.1 and 10 K is shown in Fig. 2. A clear sharp SC anomaly is observed at $T_c \approx 2.75$ K for K(Na)122 and at $T_c \approx 3.5$ K for K122 in line with the resistivity and ac susceptibility measurements. The jump height of C at T_c is found to be $\Delta C/T_c \approx 40$ mJ/mol K^2 for the K(Na)122. This value is a bit reduced from $\approx$ 46 mJ/mol K^2 for K122. A zoom into the low-T range is shown in the inset of Fig. 2. We observe a pronounced T^2-behavior in the SH for both crystals which provides a direct evidence of line nodes in the SC gap of $K_{1-x}Na_xFe_2As_2$, at least for $x \leq 0.1$ (see below). Notice that *no* kinks and/or small hump anomalies, predicted for the low-T region by weakly coupled two-band approaches [16, 17], have been observed in our measurements.

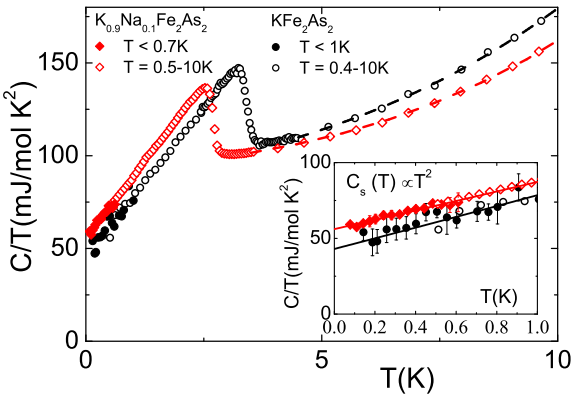

FIG. 2: (Color online) Specific heat C of KFe_2As_2 and $K_{0.9}Na_{0.1}Fe_2As_2$ plotted as C/T vs. T. Dashed lines: Fit in the normal state (see text and Eq. (S1) in Ref. 22. Inset: Zoom into the low-T region, solid lines: Fits using Eq. (3).

The T-dependence of the upper critical field, H_{c2}, of K(Na)122 obtained from SH measurements in fields $B \parallel c$ and $B \perp c$ [22] is summarized in Fig. 3. From the fit of our data use of the single-band Werthamer-Helfand-Hohenberg (WHH) theory [23] we obtain $\mu_0 H_{c2}^{\rm orb}(B \parallel c) \approx 1$ T and $\mu_0 H_{c2}^{\rm orb}(B \perp c) \approx 4.5$ T. The H_{c2} anisotropy of K(Na)122 is found to be $\Gamma = H_{c2}^{B\perp c}/H_{c2}^{B\parallel c} \approx 5$ near T_c. This value is in a good agreement with the one obtained recently for K122 [24]. The inset of Fig. 3 presents the scaled upper critical field, $\mu_0 H_{c2}/T_c^2$, as a function of the

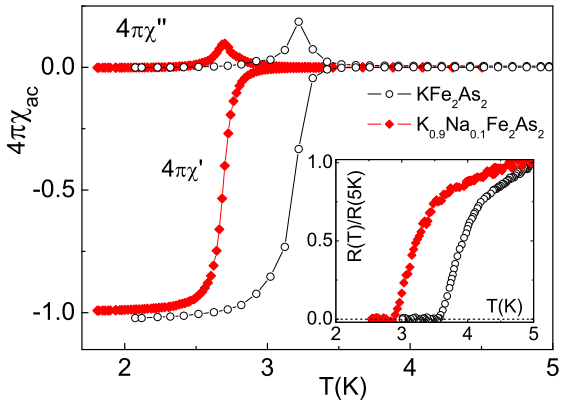

FIG. 1: (Color online) Temperature dependence of the complex volume ac susceptibility $\chi_{\rm ac} = \chi' + i\chi''$ measured with an amplitude of 5 Oe and a frequency of ν= 1 kHz, Inset: The normalized in-plane electrical resistivity measured in zero-field.

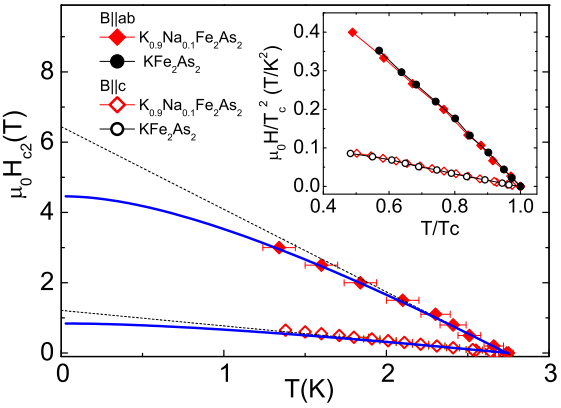

FIG. 3: (Color online) Temperature dependence of the upper critical field, H_{c2}, $K_{0.9}Na_{0.1}Fe_2As_2$. Solid lines: Theoretical curves based on the WHH model. The dashed lines depict the slopes of $H_{c2}(T)$ at T_c. Inset: The scaled upper critical fields for KFe_2As_2 [24] and $K_{0.9}Na_{0.1}Fe_2As_2$ vs. T/T_c.

reduced temperature, T/T_c, for K122 [24] and K(Na)122. The observed scaling is generally expected in the clean limit [25], where $H_{c2}(0) \propto T_c^2$.

Now, we will turn to the low-T part of the SH as one of the central points of our letter. The T-dependence of the SH in the SC state allows to determine whether the gap function possesses nodes. For instance, the exponential vanishing of C as in conventional s-wave SC is caused by the finite gap in the quasiparticle spectrum. In contrast, in the case of gap nodes quasiparticles are generated to the largest extent in the vicinity of the gap nodes. In the case of line nodes the quasiparticle excitation spectrum takes the form $E_k = \hbar\sqrt{v_{\rm F}^2 k_\perp^2 + v_\Delta^2 k_\parallel^2}$ [27, 28], where $k_\perp$ and $k_\parallel$ are wavevectors perpendicular and parallel to the FSS, respectively, $v_{\rm F}$ is the *renormalized* in-plane Fermi velocity at the position of the node, while $v_\Delta \approx \partial\Delta/\hbar\partial k$ is the slope of the gap at the node associated with the dispersion of the quasiparticles along the FS. This leads to a density of states (DOS) linear in-energy. For the two-dimensional (2D) case it reads:

$$N_{SC}(E) = \sum_i \frac{E}{\pi\hbar^2 v_{\rm F}^i v_\Delta^i}, \qquad (1)$$

where i denotes the sum over all nodes. Here, we would like to note that both materials considered are highly anisotropic, justifying the 2D approximation. The ratio of H_{c2} (in-plane vs. out-off plane) according to Fig. 3 suggests a large mass ratio $\Gamma^2 \approx 25$. This value agrees with DFT calculations for the ratio of the corresponding squared plasma frequencies [24]. Eq. (1) results in a quadratic power-law dependence $C_s \propto \alpha_{\rm sc} T^2$, with

$$\alpha_{\rm sc}({\rm mJ/mol\ K^3}) \approx 0.283 \frac{\varkappa\gamma_{\rm el}({\rm mJ/mol\ K^2})}{\Delta_0({\rm meV})} \qquad (2)$$

taken from Refs. 19, 20, 28 valid for SC in a clean-limit, where we assumed that the energy gap at zero temperature, Δ_0, is equal for all bands, while γ_{el} is a *renormalized* normal-state Sommerfeld coefficient, which is an average value over all FSS (see the Supplement for details [22]). In this context, $\varkappa$ is a dimensionless factor taking into account the anisotropy of $1/v_{\rm F}$ at the position of the nodes with respect to the averaged isotropic value. According to our preliminary *ab initio* calculations for the k-dependent DOS near the Fermi energy in dependence on the nodal direction and the expected amount of the anisotropic mass renormalization due-to anisotropic SF $0.8 \leq \varkappa \leq 1.2$. The upper bound is also in agreement with the slightly larger gap value obtained in our Eliashberg-theory based calculations (see below) than the value derived from Eq. (2).

To analyze the low-T SH data we use the ansatz:

$$C = \gamma_r T + \alpha T^2 + \beta_3 T^3, \qquad (3)$$

where the cubic term β_3 comes from phonons, which is defined from the data in the normal state (see Supplement [22]). The remaining terms stem from a magnetic cluster-glass contribution reported previously in Ref. 26 and from electronic degrees of freedom, which is the focus here. The best fit using Eq. (3) yields $\gamma_r = 43$ mJ/mol K^2 and $\alpha = 34.9$ mJ/mol K^3 for K122 and $\gamma_r = 56.1$ mJ/mol K^2 and $\alpha = 30.6$ mJ/mol K^3 for K(Na)122. It has been shown in Ref. 26 that the residual "Sommerfeld" coefficient γ_r stems mainly due to a cluster-glass phase. However, we emphasize that the T^2 contribution measured by α is not an extrinsic "glassy"contribution but stems from the generic electronic contribution in the superconducting state, only. The estimated contribution of the cluster glass amounts $\alpha_{\rm SG} \approx 2$ mJ/mol K^3 for K122 and $\alpha_{\rm SG} \approx 0$ for K(Na)122 [22, 26]. Hence, we argue that our observed large T^2 terms come from quasiparticle excitations near line nodes. The resulting coefficients are $\alpha_{\rm sc} \approx 32$ mJ/mol K^3 for K122 and $\alpha_{\rm sc} \approx 31$ mJ/mol K^3 for K(Na)122. Such a large T^2 contribution to the low T SH provides evidence of the d-wave character of the gap function.

Now, we will check whether the value of $\alpha_{\rm sc}$ can be satisfactory described by the standard d-wave mechanism on all FSS. Our analysis is based on Eq. (2), which was obtained within a BCS-like theory. But it works very well also in the case of strongly coupled cuprates [29]. Therefore, we expect its validity for pnictides, too. In addition, we analyse the relevant coupling constants with the help of the strong-coupling Eliashberg equations in the clean limit. The coupling constants $\lambda_{\rm sf}$ of the el-SF and $\lambda_{\rm ph}$ of the electron-phonon interaction together with the two bosonic spectral densities $\alpha^2(\omega)F(\omega)$ determine the gap value and T_c as well. A broad spectral density for intraband SF as obtained by recent inelastic neutron scattering measurements [5] can be described as:

$$\alpha^2 F(\omega) = \frac{\lambda_{sf}\Gamma_{sf}}{\pi} \frac{\omega}{\omega^2 + \Gamma_{\rm sf}^2}, \qquad (4)$$

where $\Gamma_{\rm sf} = 7.9$ meV. For the phonons we assume a sharp Lorentzian spectral density with a width of 0.5 meV centered at $\omega_{\rm ph} \sim 20$ meV. Notice that in our simple isotropic effective single-band model considered here for a d-wave superconducting order parameter, the el-ph coupling (EPC) drops out from the gap equation by symmetry and it enters only the equation for the Z function which describes the bosonic mass renormalization of the h-like quasiparticles [22]. Thus, here the EPC results in a slight *suppression* of T_c and Δ_0 in contrast to the $s_\pm$ case, where the superconductivity becomes stronger taking into account an intraband EPC. The SC gap and $T_{\rm c}$ calculated within Eliashberg-theory and their dependence on the SF coupling constant $\lambda_{\rm sf}$ for $\lambda_{ph} = 0$ for the sake of simplicity and also for the more realistic case, with a weak el-ph coupling constant $\lambda_{ph} \sim 0.2$ (according to density functional theory based calculations [24]) included, are shown in Fig. S2 of Ref. 22. In order to reproduce $T_{\rm c}$, $\lambda_{\phi,{\rm sf}} \sim 0.64 = 0.8\lambda_{\rm z,sf}$ should be adopted for K122, where the former describes the strength of the

paring interaction and the latter stands for the mass renormalization: see also Ref. 22. (In the isotropic s-wave case $\lambda_{\phi,\mathrm{sf}} = \lambda_{\mathrm{z,sf}}$ holds.) These values for the coupling constants together with the calculated EPC constant $\lambda_{\mathrm{ph}} \approx 0.2$ [24] yield a total coupling constant of $\lambda_{\mathrm{z,tot}} \approx 1$. As a result we get $\Delta(0)^{ET} \approx$0.75 meV (see Ref. 22 for more details), which is close to that in BCS theory $\Delta_0^{BCS} \sim 0.65$ meV obtained from the $2\Delta_0/T_c$ ratio for a d-wave superconductor in the 2D case:

$$\frac{2\Delta_0^{BCS}}{k_{\mathrm{B}}T_{\mathrm{c}}} = \frac{4\pi}{\gamma_E\sqrt{e}} \approx 4.28, \qquad (5)$$

where γ_E is the Euler constant $\gamma_E = 1.781$. The obtained $\lambda_{\mathrm{z,tot}}$ values suggest that we are in the regime of intermediate coupling and we may apply Eq. (2) to extract Δ_0. Considering the isotropic case ($\varkappa = 1$) of Eq.(2), the same gap function for all bands and using the experimental electronic linear coefficient γ_{el} =52-68 mJ/mol K^2 [26], we estimate Δ_0^{exp} in the range 0.5 - 0.6 meV, which is close to the values obtained above theoretically. It is also close to the larger gap values $\Delta_1 \approx 0.7$ to 0.8 meV obtained within effective weak-coupling two-band models for the electronically weakly connected bands [16, 17]. However, the eight times smaller second gap Δ_2 [16, 17] with a comparable partial DOS for the second effective band would produce too large α_{sc} values exceeding our experimental value by a factor of three or more. Hence, such a multiband scenario can be excluded on the basis of our study [30]. Thus, our d-wave scenario with comparable gaps with nodes in the gap function on all hole-like bands is in a good agreement with the experimental α_{sc} values. Obviously, our low-T data exclude the relevance of any full-gap scenario derived from SH data at relatively high temperature below T_c, only, such as done in Refs. 16, 24. In this context, we note that the SH jump $\Delta C/T_c\gamma_{el} \approx 0.7$ - 0.9 is close to the theoretical weak coupling value of 0.95 for a d-wave superconductor [20].

Now, we compare the experimental value of α_{sc} with that for the "octet line nodes"scenario proposed in Ref. [15]. As shown in our Supplement [22], the experimental value of α_{sc} is too large to be described by a single gap with "octet line nodes"on the middle (ζ) FSS, only, as suggested in Ref. 15. Thus, we argue that the recently proposed interpocket $s_\pm$ scenario [8] with accidental line nodes on a particular FSS, only, is rather unlikely to be realized in the bulk as probed by the SH. Therefore, despite the multi-band topology of $K_{1-x}Na_xFe_2As_2$, according to our SH data it behaves more or less like a single-band d-wave SC with corresponding line nodes on all FSS as suggested by Reid *et al.* based on a thermal-conductivity study and universal scaling arguments valid for single-band d-wave SC [11, 12] and predicted also by microscopic weak-coupling theory [3].

In summary, high-quality $K_{1-x}Na_xFe_2As_2$ (x=0,0.1) single crystals were studied by specific-heat measurements. Large T^2 contributions at low-T evidence the presence of line nodes in the superconducting gap. From the experimental value of α_{sc}, an effective gap amplitude $\Delta_0^{exp} \sim 0.5$ - 0.6 meV was estimated. This Δ_0^{exp} and T_{c} agree well with the gap value calculated within Eliashberg-theory for a one-band d-wave superconductor implying a moderately strong electron-boson coupling constant $\lambda_{\mathrm{z,tot}} \approx 1$. This suggests that all Fermi-surface sheets have comparable gap amplitudes. Our data provide direct evidence for d-wave superconductivity in a Fe-pnictide system. A detailed comparison with the cuprates might be helpful to deepen our understanding of the paring mechanism in both unconventional and still challenging superconducting families.

We thank D. Evtushinsky and V. Zabolotnyy for fruitful discussions as well as M. Deutschmann, S. Müller-Litvanyi, R. Müller, J. Werner, S. Pichl, K. Leger and S. Gass for technical support. This work was supported by the DFG through SPP 1458 and by the Emmy Noether program (WU 595/3-1 (S.W.)), and FP7-NMP-2011-EU-Japan project (No. 283204 SUPER-IRON). I.M. M.R. thank funding from RFBR (12-03-01143-a, 12-03-91674-ERA-a, 12-03-31717 mol-a), S.J. acknowledges financial support from FOM (The Netherlands), and S.W. thanks the BMBF for support in the frame of the ERA.Net RUS project.

‡ Electronic address: s.l.drechsler@ifw-dresden.de

[1] P.J. Hirschfeld *et al.*, Rep. Prog. Phys. **74**, 124508 (2011).
[2] G. R. Stewart, Rev. Mod. Phys. **83**, 1589 (2011).
[3] R. Thomale *et al.*, Phys. Rev. Lett. **107**, 117001 (2011).
[4] S. Maiti *et al.*, Phys. Rev. Lett. **107**, 147002 (2011).
[5] C.H. Lee *et al.*, Phys. Rev. Lett. **106**, 067003 (2011).
[6] A. Chubukov, Ann. Rev. Cond. Mat. Phys. **3**, 57 (2012).
[7] K. Suzuki *et al.*, Phys. Rev. B **84**, 144514 (2011).
[8] S. Maiti *et al.* Phys. Rev. B **85**, 014511 (2012).
[9] S. Avci *et al.*, Phys. Rev. B **85**, 184507 (2012).
[10] D. V. Evtushinsky *et al.*, Phys. Rev. B **79**, 054517 (2009).
[11] J. Ph. Reid *et al.*, Supercond. Sci. Technol. **25**, 084013 (2012).
[12] J. Ph. Reid *et al.*, Phys. Rev. Lett. **109**, 087001 (2012).
[13] J. K. Dong *et al.*, Phys. Rev. Lett. **104**, 087005 (2010).
[14] K. Hashimoto *et al.*, Phys. Rev. B **82**, 014526 (2010).
[15] K. Okazaki *et al.*, Science **337**, 1314 (2012).
[16] H. Fukazawa *et al.*, J. Phys. Soc. Jpn. **80**, SA118 (2011).
[17] H. Fukazawa *et al.*, J. Phys. Soc. Jpn. **78**, 083712 (2009).
[18] J. S. Kim *et al.*, Phys. Rev. B **83**, 172502 (2011).
[19] C. Kübert and P.J. Hirschfield, Solid State Comm. **105**, 459 (1998).
[20] B. Dóra and A. Virosztek, Eur. Phys. J. B **22**, 167 (2001).
[21] M. Sigrist and K. Ueda, Rev. Mod. Phys. **63**, 239 (1991).
[22] Supplement. Link to be added by the Journal.
[23] N. R. Werthamer *et al.*, Phys. Rev. **147**, 295 (1966).
[24] M. Abdel-Hafiez *et al.*, Phys. Rev. B **85**, 134533 (2012).
[25] S. V. Shulga and S.-L. Drechsler, J. Low Temp. Phys. **129**, 93 (2002).
[26] V. Grinenko *et al.*, phys. stat. sol. B, **DOI 10.1002/pssb.201200805**, 1 (2013), e-prints:

arXiv:1203.1585 and 1210.4590.
[27] A. C. Durst and P. A. Lee, Phys. Rev. B **62**, 1270 (2001).
[28] I. Vekhter *et al.*, Phys. Rev. B **64**, 064513 (2001).
[29] M. Ido *et al.*, Physica C **263**, 255 (1996).
[30] In our opinion, the lager gap Δ_1 in a simple two-gap fit with $\Delta_1 \gg \Delta_2$ applied to the relatively "high-T"SH data [16, 17], simulates the strong coupling effect, which we have included explicitly in our approach.

SUPPLEMENT

We present details of the specific heat (SH) measurements in external magnetic fields and of the analysis of data in the normal state. We also briefly sketch some aspects of the renormalization of the normal-state Sommerfeld coefficient and details of our Eliashberg-theory based calculations for T_c and the superconducting order parameter Δ_0 discussed in the main text. For the clean limit case an estimate of the coefficient α_{sc} which enters the T^2 term in the low-T SH expansion is provided for the $s_{\pm}$-scenario with accidental nodes proposed recently, too.

Specific-heat of $K_{0.9}Na_{0.1}Fe_2As_2$ (K(Na)122) in magnetic fields

The temperature dependence of the SH of a K(Na)122 single crystal in magnetic fields $B \parallel c$ (a) and $B \parallel ab$ (b) is summarized in Fig. S1. The SC jump shifts and broadens systematically to lower temperature with increasing field. The shift is more pronounced for $B \parallel c$ than for $B \perp c$ reflecting the large upper critical field anisotropy of this compound. The extracted temperature dependence of the upper critical fields for both field orientations are shown in the main text in Fig. 3. For the measurements in fields B parallel ab a small copper block was used to orient the sample. The SH of the copper block was determined in a separate measurement and subtracted from the data. However, we observed a small discrepancy between the data measured with that copper block (but subtracting its contribution afterwards) and without a copper block as can be seen in Fig. S1, which originates in the larger experimental error when using the copper block. Therefore, for the quantitative analysis of the SH we used only data measured without a copper block.

Analysis of the specific-heat in the normal state

To extract correctly α_{sc} from the experimental data shown in Fig. 2 in the main text, at first, the normal state SH for both samples has been fitted by the expression accounting for the electronic, lattice, and magnetic (due to a cluster glass (CG) phase) contributions as proposed in Ref. S1:

$$C_p = \gamma_n T + \varepsilon_{CG} T^2 + \beta_3 T^3 + \beta_5 T^5, \tag{S1}$$

where γ_n= 95(2) mJ/mol·K^2 for K(Na)122 and 89(3) mJ/mol·K^2 for KFe_2As_2 (K122) are linear contributions to the SH (denoted as *nominal* Sommerfeld coefficients) which are the sum of the standard intrinsic electronic contributions γ_{el} related to the itinerant charge carriers (quasiparticles) (the so-called Sommerfeld coefficient) and

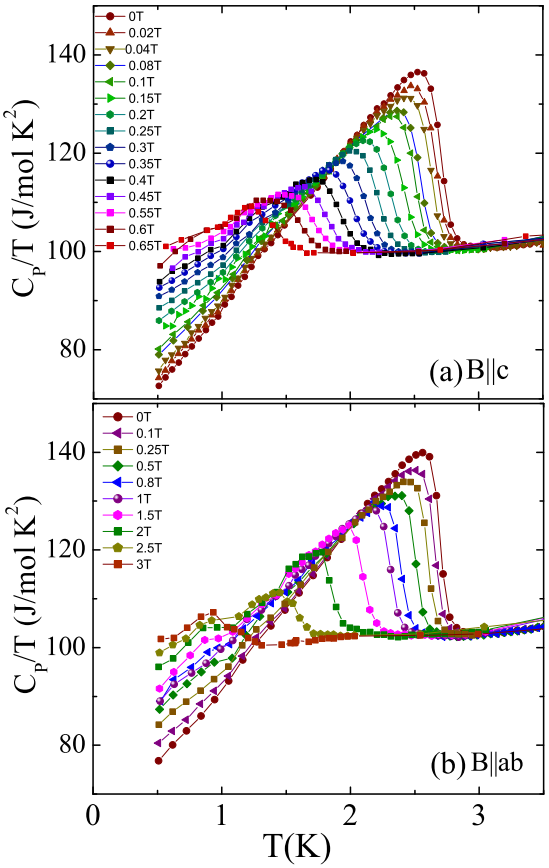

FIG. S1: Temperature dependence of the specific heat of $K_{0.9}Na_{0.1}Fe_2As_2$ in various applied magnetic fields parallel to the c axis (a) and parallel to the ab plane (b).

another linear, somewhat unusual glassy magnetic contribution γ_{CG} related to the CG-phase [S1], and $\varepsilon_{\rm CG}$ is a quadratic contribution due to the CG-phase. It was found that $\varepsilon_{\rm CG} \approx 0$ for K(Na)122 and $\varepsilon_{\rm CG} \approx 2$ mJ/mol·K^3 for K122 [S1]. Finally, the lattice contributions are $\beta_3 = 0.556$ mJ/mol·K^4 and $\beta_5 = 1.16 \cdot 10^{-3}$ mJ/mol·K^6 for K(Na)122 and $\beta_3 = 0.589$ mJ/mol·K^4 and $\beta_5 = 1.2 \cdot 10^{-3}$ mJ/mol·K^6 for K122.

Now, we briefly comment on the renormalization of the Sommerfeld coefficient due to the electron-boson interaction. The Eliashberg-theory, which we use to calculate T_c and Δ, considers the low-energy sector of characteristic bosonic energies. Within this approach the relation between the SH of the "bare" electrons γ_{el}^{η} and the renormalized quasiparticles due to electron-boson interaction γ_{el} reads:

$$\gamma_{\rm el} = \gamma_{\rm el}^{\eta}(1 + \lambda_{\rm z,tot}),$$

where $\lambda_{\rm z,tot} = \lambda_{z,sf} + \lambda_{z,ph}$ consists of two contributions: the electron-spin-fluctuation interaction $\lambda_{z,sf}$ and the electron-phonon interaction $\lambda_{\rm z,ph}$ (see also the next subsection.) This renormalization gives a factor of about two for the enhancement of the Sommerfeld coefficient and similarly for the mass in the plasma frequency which determines the penetration depth and the superconducting condensate density for $T \to 0$. The enhancement factor of the order $2.5-3$ of the Sommerfeld coefficient as compared to the LDA calculations $\gamma_{el}^{LDA} = 10.5$ mJ/mol K^3 and $\gamma_{el}^{\eta} \sim 30$ mJ/mol K^3 is due to a high-energy renormalization of the bands by self-energy effects beyond the LDA based approach seen also in the ARPES data and similarly in the optical mass which enters the Drude weight, i.e., the intraband plasma frequency at high temperature and energies as compared to the low-energy bosons included in our Eliashberg-theory based approach (for details see Refs. S2, S3, S4, S5).

Details for the d-wave Eliashberg-theory based calculations

We consider here, for the sake of simplicity, a two-dimensional (2D) single-band d-wave superconductor with a cylindrical Fermi surface parameterized by the angle θ. In general, the momentum dependence of the electron-boson spectral function for a given mode can be expanded in terms of Fermi surface harmonics

$$\alpha^2F(\omega,\theta,\theta') = \sum_{JJ'} Y_J(\theta)\alpha^2F(\omega,J,J')Y_{J'}(\theta'), \tag{S2}$$

where the functions Y_J denote the spherical harmonics. For simplicity, we assume that $\alpha^2F(\omega,\theta,\theta')$ is dominated by contributions from $J=0$ ($Y_0 \equiv Y_z = 1$) and $J=2$ ($Y_2 = Y_\phi \equiv \sqrt{2}\cos(2\theta)$) and that it is diagonal in the basis J, J'. This is the minimal set required to model d-wave superconductivity. Then the electron-boson spectral function can be parameterized via dimensionless coupling constants λ_z and λ_ϕ:

$$\alpha^2F(\nu,\theta,\theta') = \sum_i [\lambda_{i,z} + 2\lambda_{i,\phi}\cos(2\theta)\cos(2\theta')]F_i(\nu) \quad , \tag{S3}$$

where i is a mode index, $F_i(\nu) = B_i(\omega)/\left[2\int_0^\infty B_i(\nu)d\nu/\nu\right]$ is a normalized electron-boson spectral function, and $B_i(\omega)$ is the bosonic density of states. We will consider contributions from two types - a single dispersionless optical-phonon ($i=$ ph) branch and a spectrum of antiferromagnetic spin fluctuations ($i=$ sf).

It is worth to introduce:

$$\lambda_{z,\phi}(n-m) = \lambda_{z,\phi}\sum_i \int_0^\infty \frac{2\nu F_i(\nu)d\nu}{\nu^2+(\omega_n-\omega_m)^2} \quad , \tag{S4}$$

where ω_n and ω_m are fermion-Matsubara frequencies.

The set of the imaginary-axis Eliashberg-equations for a d-wave superconductor reads:

$$\phi(i\omega_n) = \frac{\pi}{\beta}\sum_m 2\lambda_\phi(m-n)\left\langle \frac{\phi(i\omega_m)\cos^2(2\theta)}{\sqrt{\omega_m^2Z^2(i\omega_m)+\phi^2(i\omega_m)\cos^2(2\theta)}}\right\rangle_\theta \quad , \tag{S5}$$

and

$$\omega_nZ(i\omega_n) = \omega_n + \frac{\pi}{\beta}\sum_m \lambda_z(m-n)\left\langle \frac{\omega_mZ(i\omega_m)}{\sqrt{\omega_m^2Z^2(i\omega_m)+\phi^2(i\omega_m)\cos^2(2\theta)}}\right\rangle_\theta \quad , \tag{S6}$$

where $\beta = 1/k_BT$ is the inverse temperature and $\langle\ldots\rangle_\theta$ denotes a Fermi surface average. The gap function is then given by $\Delta(i\omega_n) = \phi(i\omega_n)/Z(i\omega_n)$. The transition temperature T_c is determined from the highest temperature at which ϕ has a non-zero solution while the gap magnitude $\Delta(T=0)$ is approximated with a low-temperature ($T \sim 0.2$ K) value of $\Delta(i\omega_n = i\pi/\beta)$.

To describe the spin fluctuations we adopt the usual form for the bosonic density of states $B_{sf}(\nu) = \frac{\Gamma_{sf}}{\pi}\frac{\nu}{\nu^2+\Gamma_{sf}^2}$, with $\Gamma_{sf} = 7.9$ meV. For the optical-phonons we assume a narrow Lorentzian line-shape $eB_{ph}(\nu) = \frac{\Gamma_{ph}/\pi}{(\nu-\Omega_{ph})^2+\Gamma_{ph}^2} - \frac{\Gamma_{ph}/\pi}{(\nu+\Omega_{ph})^2+\Gamma_{ph}^2}$, centered at $\Omega_{ph} = 20$ meV and $\Gamma_{ph} = 0.5$ meV. We further assume that the phonons do not contribute to the d-wave pairing ($\lambda_{\phi,ph} = 0$) and we adopt the so called unbalanced scenario for d-wave superconductivity [S7], $\lambda_{\phi,sf} = 0.8\lambda_{z,sf}$. This ratio is also in good agreement with $\lambda_{s,d}$ in Ref. S8.

In Fig. S2 we plot $2\Delta(T=0)/k_BT_c$ extracted by use of this model. For λ_{sf} and $\lambda_{ph} = 0$, this ratio tends to about 4.28 (not shown in Fig. S2). Thus, the electron-phonon coupling reduces the strong-coupling corrections in this special case.

Comparison of α_{sc} for $d-$ and $s_\pm$-wave (with accidental nodes) SC order parameters

The experimental value of α_{sc} discussed in the main text is too large to be described by a gap with "octet-line nodes" on the middle (ζ) FSS, only, as suggested in Ref. S9. In fact, let us consider the ratio between α_{sc}^d for a d-wave gap with 16 nodes on all FSS having nearly equal gaps $\Delta_0 \approx 0.6$meV and α_{sc}^s for a single s-wave gap with 8 nodes on

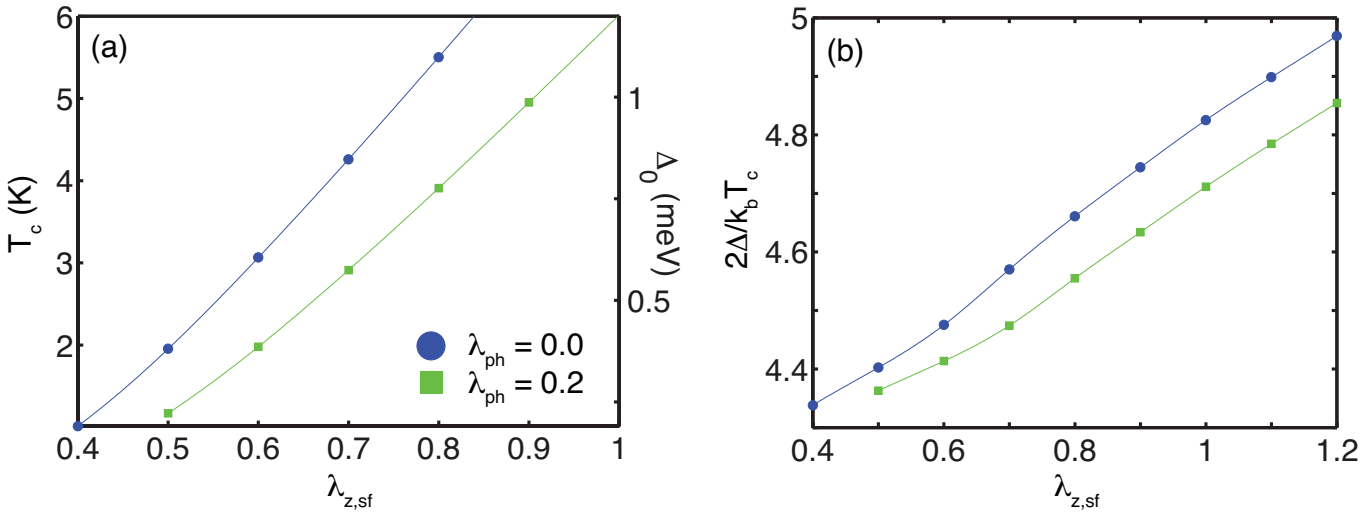

FIG. S2: (a) Superconducting gap Δ and T_c obtained from our model calculations as a function of $\lambda_{z,sf}$. (b) The corresponding ratio of $2\Delta/k_B T_c$.

a particular FSS. Using the general expression for the coefficient α_{sc} in the T^2 term entering Eqs. (1) and (2) in the main text, we have:

$$N_{SC}(E) = \sum_i \frac{E}{\pi\hbar v_F^i \partial\Delta^i/\partial k} \approx \frac{E}{\partial\Delta/\partial\theta} \sum_i \varkappa^i N^i(\varepsilon_F). \tag{S7}$$

Here, we assumed that $\partial\Delta/\partial k = \partial\Delta/\partial\theta \frac{1}{k_F}$ and then $N^i(\varepsilon_F)$ is the DOS in the normal state corresponding to the ith FSS with a node. According to the considerations given in the main text we have:

$$\alpha_{sc} \approx \frac{9}{2}\zeta(3) k_B^3 \frac{E}{\partial\Delta/\partial\theta} \sum_i \varkappa^i N^i(\varepsilon_F) \approx 0.283 \frac{\varkappa\gamma_{el}}{\Delta_0}. \tag{S8}$$

The last expression is written for the case of a d-wave SC gap ($\partial\Delta/\partial\theta = 2\Delta_0$) measured in meV and where ζ denotes Riemann's zeta function and $\zeta(3) = 1.2$. We used also that the bare Sommerfeld coefficient $\gamma_{el} = \frac{\pi^2 k_B^2}{3} N_{tot}(\varepsilon_F)$. For the sake of simplicity, we also assumed that all FSS have similar $\varkappa$ values, therefore, $\sum_i \varkappa^i N^i(\varepsilon_F) = 4\varkappa N^i(\varepsilon_F) = \varkappa N_{tot}(0)$. Finally, from Eq. (S8) for $T \ll \Delta_s^{min} \approx 1.3$ K [S9] we estimate:

$$\frac{\alpha_{sc}^d}{\alpha_{sc}^s} \approx \frac{\varkappa \sum_i N^i(\epsilon_F)(1+\lambda^i)/\partial\Delta_d/\partial\theta}{2\varkappa^\zeta N^\zeta(\epsilon_F)(1+\lambda^\zeta)/\partial\Delta_s/\partial\theta} \approx 4.5, \tag{S9}$$

where we used (according to our calculations and Ref. [S4]) that $\frac{\varkappa\sum_i N^i(\epsilon_F)(1+\lambda^i)}{\varkappa^\zeta N^\zeta(\epsilon_F)(1+\lambda^\zeta)} \sim 5$ with $\lambda^\zeta \approx \lambda^{tot}$, $\varkappa/\varkappa^\zeta \sim 1.3$, and $\partial\Delta_s/\partial\theta \approx 1.8\partial\Delta_d/\partial\theta$, where $\varkappa^\zeta$ and $\partial\Delta_s/\partial\theta$ have been calculated at the nodal directions of the ζ FSS according to the data given in Ref. S9. For the physical consequences of this estimated ratio with respect to the symmetry of the superconducting order parameter, see the main text.

‡ Electronic address: s.l.drechsler@ifw-dresden.de

[S1] V. Grinenko *et al.*, phys. stat. sol. B, **DOI 10.1002/pssb.201200805**, 1 (2013), e-prints: arXiv:1203.1585 and 1210.4590.
[S2] M. Abdel-Hafiez *et al.*, Phys. Rev. B **85**, 134533 (2012).
[S3] W. Lee and D. Rainer, Z. Phys. **73** , 149 (1976).
[S4] K. Hashimoto *et al.*, Phys. Rev. B **82**, 014526 (2010).
[S5] S.-L. Drechsler *et al.*, Phys. Rev. Lett. **101** 257004 (2008); - Physica C **470**, Supplement **1** S332-S333 2(2010).
[S6] See for example J.P. Carbotte and C. Jiang, Phys. Rev. B **48**, 4231 (1993).
[S7] E. Cappellutti and G.A. Ummarino, Phys. Rev. B **76**, 104522 (2007).
[S8] H. Ikeda, R. Arita, and J. Kunesh, Phys. Rev. B **81**, 054502 (2010).
[S9] K. Okazaki *et al.*, Science **337**, 1314 (2012).